Singly ionized first-row dimers and hydrides calculated with the fully-numerical density-functional program NUMOL

R. Merkle, A. Savin, and H. Preuss
Institut für Theoretische Chemie der Universität Stuttgart, Pfaffenwaldring 55, D-W-7000 Stuttgart 80, Germany

(Received 24 August 1992; accepted 10 September 1992)

Gradient corrected density functionals yield average errors in the ionization potentials of 0.3–0.8 eV. The average errors in the dissociation energies of the diatomic cations are similar to the corresponding errors of the neutral molecules, i.e., 0.2–0.6 eV. The wrong behavior of the potential curves of the dimer cations at large distances calculated with these functionals does not affect the accuracy of D_e.

I. INTRODUCTION

For molecules, the bond dissociation energies are an important quantity, and in the collection of diatomic molecules that we treat here, different types of bonding and strengths of bonds can be found. The good results of density-functional theory in calculating dissociation energies have been explained by the correct dissociation of the charge density along the potential curve.[1] But these two effects must not always occur simultanously. Slater[2] remarks that for example in a NaCl molecule at large distance charge must be transferred from Na to Cl to get the minimum of the total energy. In a calculation using the local spin density approximation (LDA), the minimum is reached for the partially ionic pair $\mathrm{Na}^{+0.4}\mathrm{Cl}^{-0.4}$.[3] When we look at the dimer cations X_2^+ at large interatomic distances, we find that the system $X^{+0.5}X^{+0.5}$ with equally distributed charge has clearly the lower energy compared with the observed dissociation products $X+X^+$. This phenomenon shows that a proper balance of Coulomb and exchange-correlation energies is not maintained at large interatomic distances in the density-functional methods we used. The Coulomb repulsion between the electrons is dominant and favors the distribution of the charge of a cation on both atoms.

II. THEORY

In the Kohn–Sham density-functional theory[4] the total energy is calculated as follows:

$$E=T_s+\int v\rho+\frac{1}{2}\int\int\frac{\rho(1)\rho(2)}{r_{12}}+E_{\mathrm{XC}}, \tag{1}$$

$T_s=-\Sigma\frac{1}{2}\nabla^2\psi_i$ is the kinetic energy of the noninteracting reference system that yields the same electronic density

$$\rho=\sum_i|\psi_i|^2 \tag{2}$$

as the system with all electron–electron interactions. The Kohn–Sham orbitals ψ_i are calculated from

$$-\tfrac{1}{2}\nabla^2\psi_i+v_{\mathrm{eff}}\psi_i=\epsilon_i\psi_i, \tag{3}$$

$$v_{\mathrm{eff}}=v_{\mathrm{nuc}}+\int\frac{\rho(2)}{r_{12}}d^3r_2+\frac{\delta E_{\mathrm{XC}}}{\delta\rho}. \tag{4}$$

$\int v\rho$ and $\frac{1}{2}\int\int[\rho(1)\rho(2)/r_{12}]$ represent the Coulomb interaction between nuclei and electrons and the electrons with each other, while $E_{\mathrm{XC}}(\rho)$ is the exchange-correlation energy. Of the several approaches for the exchange-correlation functional $E_{\mathrm{XC}}(\rho)$ we will mention these that are used in the present paper.

One of the simplest ways of getting $E_{\mathrm{XC}}(\rho)$ is the local spin density approach

$$E_{\mathrm{XC}}(\rho)=\int\rho\epsilon_{\mathrm{XC}}(\rho_\alpha,\rho_\beta)d^3r, \tag{5}$$

where $\epsilon_{\mathrm{XC}}(\rho_\alpha,\rho_\beta)$ is the exchange-correlation energy per electron in the uniform electron gas with the densities ρ_α,ρ_β (see Appendix for explicit formulas). Naturally the uniform electron gas is not a very good reference system for atoms and molecules with nonuniform electronic density. A successful expression for E_{XC} was developed by Becke[5] and contains a gradient correction for the exchange part (see Appendix). Results of this approach will be denoted BX.

In their generalized gradient approximation (GGA91) Perdew and Wang[6] use a correction for exchange similar to that of Becke, and correct the correlation energy with an expression derived from a modeled correlation hole (see Appendix).

III. COMPUTATIONAL DETAILS

In this work we performed calculations for the diatomic molecules and their ions at the experimental equilibrium distance[7,8,16] with the fully-numerical basis-set-free density-functional program NUMOL which was developed by Becke[9] (for further details). Only the valence orbitals are optimized, the core orbitals are transferred from numerical atomic calculations using the LDA. During the iterations v_{eff} is calculated at the LDA level, after the last step the gradient corrections are applied for obtaining E_{XC}. Open-shell systems are treated in the spin-unrestricted formalism.

The molecular orbitals were occupied in such a way (broken occupation numbers if necessary) that the molecules had cylindrical symmetry. The difference to the system treated with broken symmetry is for example for C_2^+ 0.04 eV (LDA) and 0.17 eV (BX). For the dimer cations O_2^+ and F_2^+ calculated with broken symmetry extensive rearrangements in the π orbitals take place (about four times more iterarions necessary for convergence than usually) and the resulting binding energy is 0.5 and 2.5 eV larger, respectively.

For calculating the dissociation energies, atomic energies are also needed. Unfortunately, approximate density functionals do not yield the same energy for the densities obtained from different degenerate states. Spherical atoms would give values different from that obtained with the molecules at large interatomic distances. While the latter choice seems natural to use with potential curves, it has the disadvantage of giving different atomic reference values for different molecules. We thus made a compromise by using a set of values from nonspherical atoms and ions (B,C^+:p_z;C,N^+:p_x,p_z;O,F^+:p_x,p_y,p_z^2;F:p_x^2,p_y^2,p_z). This occupation lowers the energy with respect to the spherical atoms (B: 0.07/0.24/0.19; C: 0.04/0.22/0.16; O: 0.18/0.46/0.45; F: 0.04/0.32/0.31 eV; LDA/BX/GGA91 values, respectively).[10,11]

IV. DIMER CATIONS AT LARGE DISTANCES

When a molecule is formed, charge is shifted in space until the minimum of the energy is reached. In density functional theory this happens also for molecules at large interatomic distances that should be rather regarded as seperate, only weakly interacting atoms and ions. The exact density functional changes linearly with the (fractional) occupation in a state intermediate between an atom A and its ion A^+ (Ref. 12) and thus no energy change will be present when redistributing the positive charge between A and A^+. This is not the case for most approximate density functionals like the ones used in this paper. Here the fragments with a noninteger number of electrons have a lower energy than the physically correct atoms and ions with integer charge. This effect is related to the nonlinearity of parts of the energy functional as $\int\int[\rho(1)\rho(2)/2r_{12}]$ or E_{XC}. We will illustrate this for the Coulomb term.

Removing a charge $\Delta\rho_A$ only from atom A in a homonuclear dimer X_A–X_B at large interatomic distance, the Coulomb term yields

$$\int\int \frac{\rho_A^2+\rho_B^2+2\rho_A\Delta\rho_A+(\Delta\rho_A)^2}{2r_{12}},$$

where ρ_A and ρ_B are the densities on atoms A and B, respectively. Keeping only the fraction $\alpha\Delta\rho_A$ on atom A and transferring the remaining fraction on atom B, giving $\beta\Delta\rho_B$ $(\alpha+\beta=1)$ yields

$$\int\int \frac{\rho_A^2+\rho_B^2+\alpha^2(\Delta\rho_A)^2+\beta^2(\Delta\rho_B)^2+2\alpha\rho_A\Delta\rho_A+2\beta\rho_B\Delta\rho_B}{2r_{12}}.$$

Considering $\int\int[\rho_A\Delta\rho_A/r_{12}]=\int\int[\rho_B\Delta\rho_B/r_{12}]$ and $\int\int[(\Delta\rho_A)^2/r_{12}]=\int\int(\Delta\rho_B)^2/r_{12}$, the difference between these terms is a contribution to the Coulomb energy of

$$\int\int \frac{(\alpha^2+\beta^2-1)(\Delta\rho_A)^2}{2r_{12}}.$$

This contribution becomes minimal for $\alpha=\beta=1/2$ in the case of X_2^+ molecules and favors the equal distribution of ionic charge on both atoms even for large interatomic distances.

TABLE I. Dimer cations at large interatomic distance. Energy difference $\Delta=E_B(A)+E_B(A^+)-E_B(A_2^+,20\ \text{Å})$ between the separated atom and ion and the dimer cation at 20 Å (in eV), using LDA, BX, and GGA91 density functionals.

Molecule	Δ_{LDA}	Δ_{BX}	Δ_{GGA91}
H_2^+	2.54	2.77	2.69
He_2^+	4.10	4.42	3.95
Li_2^+	0.93	0.99	0.99
Be_2^+	1.53	1.61	1.53
B_2^+	2.18	2.18	2.16
C_2^+	2.70	2.56	2.58
N_2^+	3.22	3.10	3.11
O_2^+	3.19	3.16	3.11
F_2^+	3.65	3.40	3.39

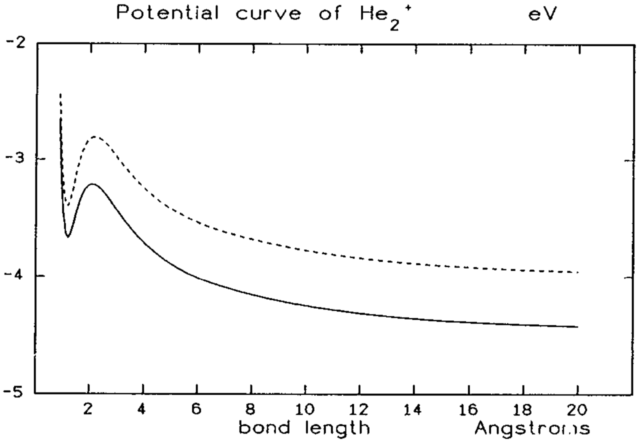

FIG. 1. Potential curve of He_2^+ (in eV; 0 eV=He+He$^+$). Solid line, BX; dashed line, GGA91.

TABLE II. Calculated dissociation energies (D) and ionization potentials (IP) in eV[a] using LDA, BX, and GGA91 density functionals.

Molecule	D_{LDA}	D_{BX}	D_{GGA91}	$\mathrm{IP}_{\mathrm{LDA}}$	$\mathrm{IP}_{\mathrm{BX}}$	$\mathrm{IP}_{\mathrm{GGA91}}$	Ion	D_{LDA}	D_{BX}	D_{GGA91}
LiH $1\Sigma^1$	2.63	2.75	2.36	7.87	8.44	7.81	$\mathrm{LiH}^+\ {}^2\Sigma^+$	0.21	0.15	0.06
BeH ${}^2\Sigma^+$	2.61	2.62	2.45	8.33	8.78	8.48	$\mathrm{BeH}^+\ {}^1\Sigma^+$	3.31	3.23	3.03
BH ${}^1\Sigma^+$	3.90	3.77	3.56	9.68	10.12	9.63	$\mathrm{BH}^+\ {}^2\Sigma^+$	2.85	2.75	2.66
CH ${}^2\Pi_r$	3.98	3.66	3.56	11.03	11.16	10.65	$\mathrm{CH}^+\ {}^1\Sigma^+$	4.64	4.40	4.23
NH ${}^3\Sigma^-$	4.14	3.96	3.85	13.96	14.24	13.99	$\mathrm{NH}^+\ {}^2\Pi_r$	3.21	3.84	3.49
OH ${}^2\Pi_i$	5.34	4.59	4.58	13.37	13.50	13.05	$\mathrm{OH}^+\ {}^3\Sigma^-$	5.00	5.21	5.16
FH ${}^1\Sigma^+$	7.03	6.16	6.21	16.57	16.89	16.47	$\mathrm{FH}^+\ {}^2\Pi_i$	3.48	3.49	3.37
							$\mathrm{He}_2^+\ {}^2\Sigma_u^+$	3.67	3.59	3.34
$\mathrm{Li}_2\ {}^1\Sigma_g^+$	1.03	0.94	0.93	5.22	5.47	5.24	$\mathrm{Li}_2^+\ {}^2\Sigma_g^+$	1.28	1.30	1.32
$\mathrm{Be}_2\ {}^1\Sigma_g^+$	0.56	0.22	0.44	7.06	7.37	7.03	$\mathrm{Be}_2^+\ {}^2\Sigma_u^+$	2.52	2.34	2.48
$\mathrm{B}_2\ {}^3\Sigma_g^-$	3.85	2.77	3.33	9.75	9.52	9.50	$\mathrm{B}_2^+\ {}^2\Sigma_g^+$	2.75	2.34	2.56
$\mathrm{C}_2\ {}^1\Sigma_g^+$	7.27	5.64	6.23	12.68	12.81	12.53	$\mathrm{C}_2^+\ {}^2\Pi_u$	6.28	4.73	5.32
$\mathrm{N}_2\ {}^1\Sigma_g^+$	11.62	10.18	10.56	15.63	15.88	15.47	$\mathrm{N}_2^+\ {}^2\Sigma_g^+$	11.00	9.35	9.90
$\mathrm{O}_2\ {}^3\Sigma_g^-$	7.59	5.53	6.24	12.32	12.80	12.39	$\mathrm{O}_2^+\ {}^2\Pi_g$	9.28	7.44	7.99
$\mathrm{F}_2\ {}^1\Sigma_g^+$	3.38	1.85	2.33	15.36	15.36	15.87	$\mathrm{F}_2^+\ {}^2\Sigma_g^+$	5.98	4.24	4.72

Atom	$\mathrm{IP}^{\mathrm{b}}_{\mathrm{LDA}}$	$\mathrm{IP}^{\mathrm{b}}_{\mathrm{BX}}$	$\mathrm{IP}^{\mathrm{b}}_{\mathrm{GGA91}}$
Li ${}^2S$	5.48	5.83	5.63
Be ${}^1S$	9.03	9.48	9.07
B ${}^2P$	8.58	8.86	8.55
C ${}^3P$	11.76	12.05	11.75
N ${}^4S$	14.92	15.22	15.00
O ${}^3P$	13.90	14.33	13.75
F ${}^2P$	18.06	18.45	17.95

[a] Data for most of the neutral molecules and atomic systems are also presented in Refs. 15 and 11 and are given here only for completeness.

[b] IP from spherical atoms to spherical ions.

This Coulomb term is compensated by a corresponding exchange-correlation term in the exact density functional. With approximate forms of the latter one can only expect an incomplete cancellation. For the density functionals studied here one always observes a dominance of the Coulomb term. A discussion of the possibilities of correcting this error is given by Perdew[13] (for some recent advances see Ref. 14).

The energy differences of ~1–4 eV that are gained in the systems $X^{+0.5}+X^{+0.5}$ at a distance of 20 Å with respect to $X+X^+$ are shown in Table I. They rise with the compactness of the atoms along the row. We would like to stress that here energy lowering cannot be used as a criterion for obtaining the solution with broken symmetry ($X+X^+$).

Only for He_2^+ the energy difference exceeds the dissociation energy of 2.5 eV. The potential curve of this molecule (see Fig. 1, 0 eV=He+He$^+$) calculated with BX and GGA91 and equal charge distribution has a well of 0.4 eV before it becomes a Coulomb repulsion curve of two $X^{+0.5}$ at large distance. The turning point is at about twice the value of R_e. The curves of the other dimer cations also become a Coulomb curve at large distances, but the global energy minimum remains at R_e. As we shall see in the comparison of the errors of the dissociation energies of the dimers and dimer cations, this misbehavior of the potential curve quite near the equilibrium bond distance does not influence the accuracy of D_e very much.

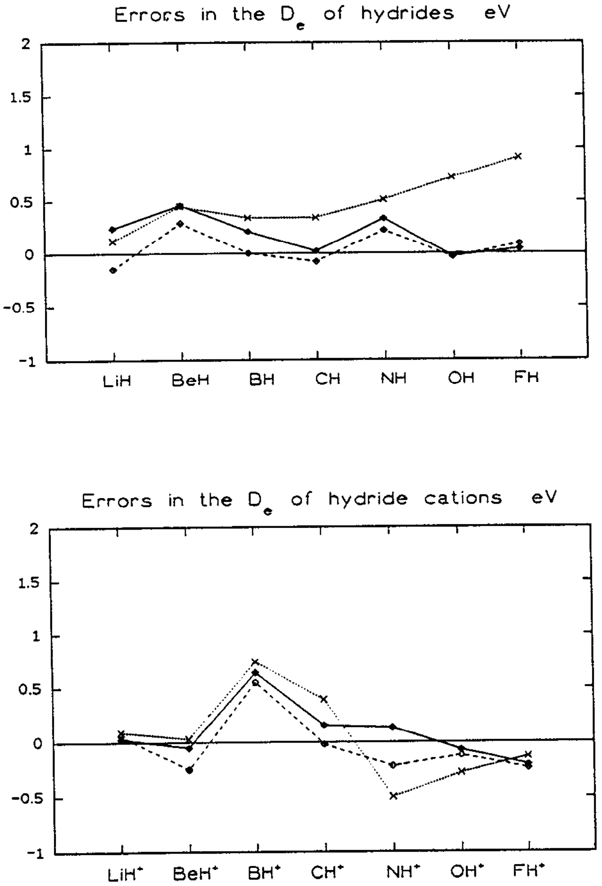

FIG. 2. Errors in the dissociation energies of the hydrides and their cations (in eV). Dotted line, LDA; solid line, BX; dashed line, GGA91.

V. RESULTS

In Table II we list our calculated values. Most of the values for the neutral molecules were already published by Becke[15] and Perdew *et al.*[11] We include them in our discussion for completeness. The errors of the calculated data are defined with respect to the experimental values collected in Ref. 7. In Fig. 2 we show the errors $\Delta D_e = D_e^{\text{calc}} - D_e^{\text{exp}}$ in the dissociation energies of the hydrides and their cations The gradient corrections lower the average errors ΔD_e of the hydrides and hydride cations from ~0.5 and 0.3 eV, respectively, using LDA to 0.1–0.2 eV. The largest error with all three approximations is found for BH^+ with 0.6–0.7 eV.

While no systematical trend in the errors can be seen for the hydrides, the ΔD_e(LDA) of the dimers and dimer cations (Fig. 3) rise in the second half of the row, being maximal for F_2^+ with 2.6 eV. This observation could be related to effects of near-degeneracy that are not completely recovered in LDA. The gradient correction approaches yield better results with maximal errors for F_2^+ of 0.8 and 1.3 eV. The average errors are 0.3 eV/0.4 eV (BX) and 0.5 eV/0.6 eV (GGA91) for the dimers and their cations, respectively. The incorrect dissociation of the dimer cations with the density functionals mentioned above does not seem to influence the dissociation energies much; the errors are of the same order of magnitude for X_2 and X_2^+. For most molecules the gradient-corrected functionals yield significantly better dissociation energies.

When we look at the ionization potentials of the atoms, hydrides, and dimers (see Fig. 4), LDA and GGA91 show average errors $\Delta IP = IP^{\text{calc}} - IP^{\text{exp}}$ of 0.2–0.4 eV. The BX ionization potentials run almost parallel to the GGA91 values, but are generally 0.2–0.4 eV larger, and so the BX values differ from the experimental data by 0.4–0.8 eV.

Although configuration interaction (CI) calculations yield correct potential curves, the errors in the dissociation energies and ionization potentials can be of the same order

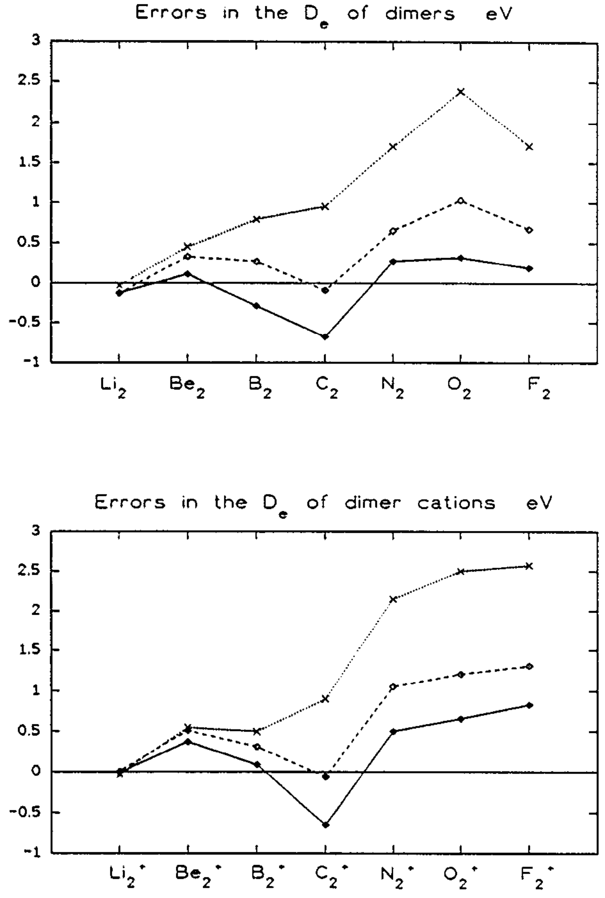

FIG. 3. Errors in the dissociation energies of the dimers and their cations (in eV). Dotted line, LDA; solid line, BX; dashed line, GGA91.

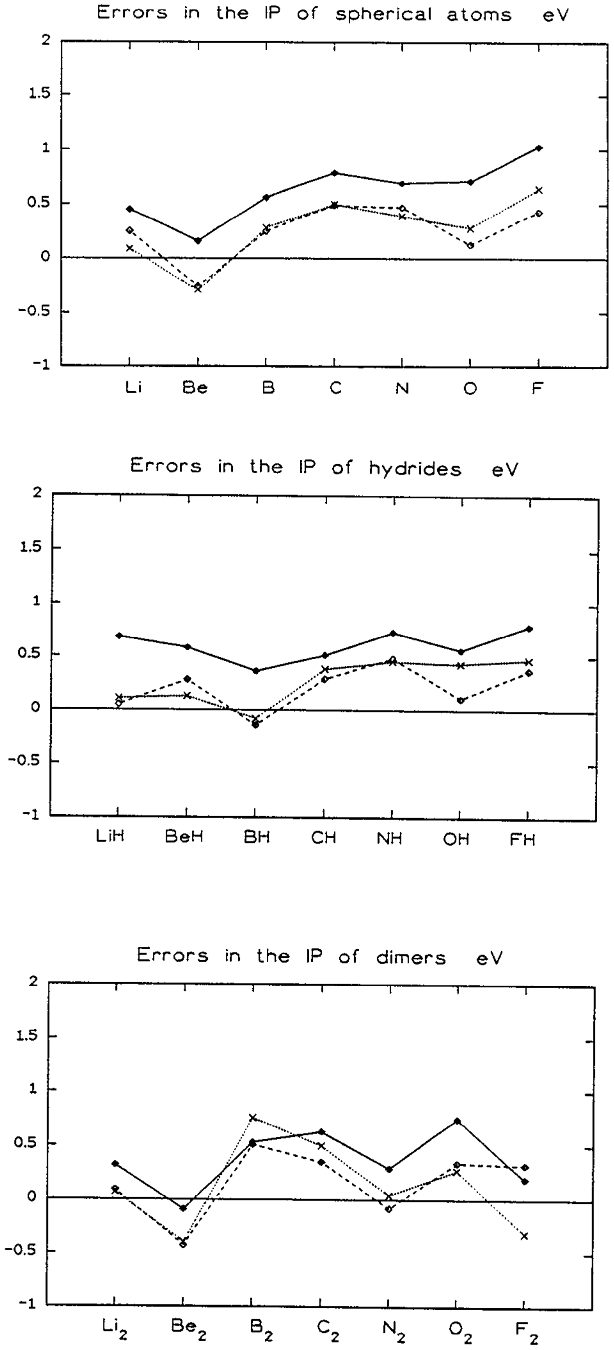

FIG. 4. Errors in the ionization potentials of atoms, hydrides, and dimers (in eV). Dotted line, LDA; solid line, BX; dashed line, GGA91.

of magnitude as with the density functionals. In additional CI calculations[17,18,19] for the dimers B_2 to F_2 and their cations we found average errors in D_e of 1.1 eV and in IP of 0.3 eV, but with reversed sign (i.e., the calculated values are too low).

VI. CONCLUSION

The calculated values for dissociation energies and ionization potentials are usually too large, i.e., the electron richer systems are stabilized more by the used density functionals than the systems with more distributed or fewer electrons. While the exchange-only gradient correction of Becke yields the better dissociation energies for the dimers and their ions, the generalized gradient approximation of Perdew and Wang works better for the ionization potentials. The wrong behavior of the density functional energies for the dimer cations at large distances does not affect the accuracy of the D_e at equilibrium bond lengths.

ACKNOWLEDGMENTS

We are grateful to Professor A. D. Becke for giving us the program NUMOL and to Professor J. P. Perdew for sending us the subroutines for calculating the GGA91 density functional. We would like to thank Professor H.-J. Werner for making available the program MOLPRO. We would also like to thank Professors A. D. Becke, J. P. Perdew, and H. Stoll for comments on the manuscript.

APPENDIX

(1) Local spin density approximation (LDA). Exchange energy

$$\epsilon_{\mathrm{X}}^{\mathrm{LDA}}=-\frac{3}{2}\left(\frac{3}{4\pi}\right)^{1/3}\int\rho_\alpha^{4/3}+\rho_\beta^{4/3}d^3r.$$

Correlation energy

$$E_{\mathrm{C}}^{\mathrm{LDA}}=\int\rho\epsilon_{\mathrm{C}}^{\mathrm{LDA}}(\rho_\alpha,\rho_\beta)d^3v,$$

$$E_{\mathrm{C}}^{\mathrm{LDA}}=\epsilon^U(1-f\zeta^4)+\epsilon^P f\zeta^4+\alpha_c f(1-\zeta^4)/d,$$

$$f=[(1+\zeta)^{4/3}+(1-\zeta)^{4/3}-2]/\gamma,$$

$$\gamma=0.519\,842\,1,\quad d=1.709\,921,$$

$$\epsilon^P=-2a_{02}(1+a_{12}r_s)\times\ln\left[1+\frac{1}{2a_{02}(b_{12}x+b_{22}x^2+b_{32}x^3+b_{42}x^4)}\right],$$

$$\epsilon^U=-2a_{01}(1+a_{11}r_s)\times\ln\left[1+\frac{1}{2a_{01}(b_{11}x+b_{21}x^2+b_{31}x^3+b_{41}x^4)}\right],$$

$$\alpha_c=-2a_{03}(1+a_{13}r_s)\times\ln\left[1+\frac{1}{2a_{03}(b_{13}x+b_{23}x^2+b_{33}x^3+b_{43}x^4)}\right],$$

$$x=r_s^{1/2},\quad r_s=\left(\frac{3}{4\pi\rho}\right)^{1/3},\quad \zeta=(\rho_\alpha-\rho_\beta)/\rho,$$

$$a_{01}=0.031\,097,\quad a_{02}=0.015\,545\,35,\quad a_{03}=0.016\,886\,9,$$

$$a_{11}=0.213\,70,\quad a_{12}=0.205\,48,\quad a_{13}=0.111\,25,$$

$$b_{11}=7.595\,7,\quad b_{12}=14.118\,9,\quad b_{13}=10.357,$$

$$b_{21}=3.587\,6,\quad b_{22}=6.197\,7,\quad b_{23}=3.623\,1,$$

$$b_{31}=1.638\,2,\quad b_{32}=3.366\,2,\quad b_{33}=0.880\,26,$$

$$b_{41}=0.492\,94,\quad b_{42}=0.625\,17,\quad b_{43}=0.496\,71.$$

(2) Becke gradient correction for exchange (BX)

$$E_{\mathrm{X}}^{\mathrm{BX}}=E_{\mathrm{X}}^{\mathrm{LDA}}-\sum_\sigma 0.0042\times\int\frac{\rho_\sigma^{4/3}x_\sigma^2}{1+0.0252x_\sigma\,\mathrm{arsinh}(x_\sigma)}d^3r,$$

$$x_\sigma=\frac{|\nabla\rho_\sigma|}{\rho^{4/3}},\quad \sigma=\text{spin }\alpha\text{ or spin }\beta.$$

(3) Generalized gradient approximation (GGA91). Exchange energy

$$E_{\mathrm{X}}^{\mathrm{GGA91}}=E_{\mathrm{X}}^{\mathrm{LDA}}+\sum_\sigma 0.738\,558\,8\cdot 2^{1/3}\times\int\rho_\sigma^{4/3}[F(s)-1]d^3r,$$

$$F(s)=\frac{1+0.196\,45s\cdot\mathrm{arsinh}(7.7956s)+(0.2743-0.1508e^{-100s^2})s^2}{1+0.196\,45s*\mathrm{arsinh}(7.7965s)+0.004s^4},$$

$$s=(3\pi^2)^{-1/3}\frac{|\nabla\rho_\sigma|}{\rho_\sigma^{4/3}},$$

σ=spin α or spin β.

Correlation energy

$$E_{\mathrm{C}}^{\mathrm{GGA91}}=E_{\mathrm{C}}^{\mathrm{LDA}}+\int(H_0+H_1)\rho d^3r,$$

$$H_0=g^3\frac{\beta^2}{2\alpha}\ln\left(1+\frac{2\alpha}{\beta}\frac{t^2+At^4}{1+At^2+A^2t^4}\right),$$

$$H_1=15.7559(\mathrm{C}_c-0.003\,521)g^3t^2e^{-100g^4(k_s^2t^2/k_{\mathrm{F}}^2)},$$

$$k_F=(3\pi\rho)^{1/3},\quad k_s=(4k_F/\pi)^{1/2},\quad r_s=\left(\frac{3}{4\pi\rho}\right)^{1/3},$$

$$\zeta=(\rho_\alpha-\rho_\beta)/\rho,\quad g=[(1+\zeta)^{2/3}+(1-\zeta)^{2/3}]/2,$$

$$t^2=(\nabla\rho)^2/4g^2k_s^2\rho^2,\quad A=\frac{2\alpha}{\beta}\frac{1}{e^{2\alpha\epsilon_c/(g^3\beta^2)}-1},$$

$$\alpha=0.09,\quad \beta=15.755\,9\cdot 0.004\,235,$$

$$\mathrm{C}_c=\frac{c_1+c_2r_s+c_3r_s^2}{1+c_4r_s+c_5r_s^2+c_6r_s^3}-c_x,\quad c_x=-0.001\,667\,212,$$

$$c_1=0.002\,568,\quad c_2=0.023\,266,\quad c_3=7.389\cdot 10^{-6},$$

$$c_4=8.723,\quad c_5=0.472,\quad c_6=7.389\cdot 10^{-2}.$$

---

[1] M. Cook and M. Karplus, J. Phys. Chem. **91**, 31 (1987).

[2] J. C. Slater, *The Self-Consistent Field for Molecules and Solids* (McGraw-Hill, New York, 1974), Vol. 4.

[3] J. P. Perdew, in *Density Functional Methods in Physics*, edited by R. M. Dreizler and J. da Providencia (Plenum, New York and London, 1985), p. 301

[4] W. Kohn and L. Sham, Phys. Rev. A **140**, 1133 (1965).

[5] A. D. Becke, Phys. Rev. A **38**, 3098 (1988).

[6] J. P. Perdew, in *Electronic Structure of Solids '91*, edited by P. Ziesche and H. Eschring (Akademie, Berlin, 1991); Physica B **172**, 1 (1991); J. P. Perdew and Y. Wang, Phys. Rev. B **45**, 13244 (1992); and unpublished.

[7] For experimental data see Table I in Ref. 16; data for He_2^+ from Ref. 8, R_e=1.08 Å, D_e=2.47 eV.

[8] A. A. Radzig and B. M. Smirnov, *Reference Data on Atoms, Molecules, and Ions* (Springer, Berlin, 1985).

[9] A. D. Becke, Int. J. Quantum Chem. Symp. **23**, 599 (1989); A. D. Becke and R. M. Dickson, J. Chem. Phys. **92**, 3610 (1990).

[10] A. D. Becke (private communication).

[11] J. P. Perdew, J. A. Chevary, S. H. Vosko, K. A. Jackson, M. R. Pederson, D. J. Singh, and C. Fiolhais, Phys. Rev. B (to be published). The density functionals are applied on the Hartree–Fock ground state density.

[12] J. P. Perdew, R. G. Parr, M. Levy, and J. L. Balduz, Phys. Rev. Lett. **49**, 1691 (1982).

[13] J. P. Perdew, Adv. Quantum Chem. **21**, 113 (1990).

[14] J. B. Krieger and Y. Li, Phys. Rev. A **45**, 101 (1992).

[15] A. D. Becke (to be published).

[16] R. Merkle, A. Savin, and H. Preuss, Chem. Phys. Lett. **194**, 32 (1992).

[17] The CI calculations were performed with the program MOLPRO [Hartree–Fock part by W. Meyer and H.-J. Werner, CI calculation by H.-J. Werner and P. J. Knowles (Ref. 18)], including all excitations in valence space (1*s* and 2*s* orbitals kept closed), basis (13*s*,8*p*,2*d*) contracted to [7*s*,3*p*,2*d*] from Ref. 19.

[18] H.-J. Werner and P. J. Knowles, J. Chem. Phys. **89**, 5803 (1988); P. J. Knowles and H.-J. Werner, Chem. Phys. Lett. **145**, 514 (1988).

[19] G. C. Lie and E. Clementi, J. Chem. Phys. **60**, 1275 (1974).